EUROPEAN ORGANIZATION FOR NUCLEAR RESEARCH (CERN)

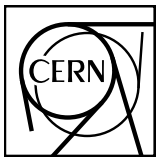

CERN-EP-2024-220
23 August 2024

Search for $B^{*0}_{(s)} \to \mu^+\mu^-$ in $B_c^+ \to \pi^+\mu^+\mu^-$ decays

LHCb collaboration[†]

Abstract

A search for the very rare $B^{*0} \to \mu^+\mu^-$ and $B_s^{*0} \to \mu^+\mu^-$ decays is conducted by analysing the $B_c^+ \to \pi^+\mu^+\mu^-$ process. The analysis uses proton-proton collision data collected with the LHCb detector between 2011 and 2018, corresponding to an integrated luminosity of $9\,\text{fb}^{-1}$. The signal signatures correspond to simultaneous peaks in the $\mu^+\mu^-$ and $\pi^+\mu^+\mu^-$ invariant masses. No evidence for an excess of events over background is observed for either signal decay mode. Upper limits at the 90% confidence level are set on the branching fractions relative to that for $B_c^+ \to J/\psi\pi^+$ decays,

$$\mathcal{R}_{B^{*0}(\mu^+\mu^-)\pi^+/J/\psi\pi^+} < 3.8 \times 10^{-5} \quad \text{and}$$
$$\mathcal{R}_{B_s^{*0}(\mu^+\mu^-)\pi^+/J/\psi\pi^+} < 5.0 \times 10^{-5}\,.$$

Submitted to Eur. Phys. J. C

[†]Authors are listed at the end of this paper.

1 Introduction

Weak decays of the B^{*0} and B_s^{*0} excited vector mesons into leptonic final states offer the opportunity to search for possible deviations from Standard Model (SM) expectations. Unlike the weak leptonic decays of the B^0 and B_s^0 pseudoscalar mesons, the decays of excited vector mesons are not suppressed by the chiral structure of the SM weak interaction [1–3]. However, since the $B_{(s)}^{*0}$ mesons decay predominantly through the electromagnetic interaction, the branching fractions for their weak leptonic decays are highly suppressed in the SM. For example, the $B_s^{*0} \to \mu^+\mu^-$ branching fraction is expected in the SM to be around 10^{-11} [2, 3], but could be enhanced due to physics beyond the SM. The impact of particular extensions of the SM on the leptonic decays of B^{*0} and B_s^{*0} mesons has been investigated in Refs. [4–8].

Many experimental studies of the $B_{(s)}^0$ leptonic decays have been performed. Recent results include measurements of the $B_s^0 \to \mu^+\mu^-$ branching fraction and limits on the $B^0 \to \mu^+\mu^-$ rate that are consistent with SM expectations [9–12], as well as limits on the rates of $B_{(s)}^0 \to e^+e^-$ and $B_{(s)}^0 \to \tau^+\tau^-$ decays [13, 14]. However, there has not yet been any search for a $B_{(s)}^{*0} \to \ell^+\ell^-$ decay mode. In this paper, the first search for the $B^{*0} \to \mu^+\mu^-$ and $B_s^{*0} \to \mu^+\mu^-$ decays is presented. The analysis is based on the data samples collected with the LHCb detector between 2011 and 2018, corresponding to an integrated luminosity of $9\,\text{fb}^{-1}$ of proton-proton (pp) collisions at centre-of-mass energies of 7, 8 and 13 TeV. As discussed in Ref. [15], searches via prompt $B_{(s)}^{*0}$ production in LHC collisions are expected to be limited by the large amount of background from pp interactions. The search is therefore performed via the $B_c^+ \to B_{(s)}^{*0}\pi^+$, $B_{(s)}^{*0} \to \mu^+\mu^-$ decay chain, subsequently denoted as $B_c^+ \to B_{(s)}^{*0}(\mu^+\mu^-)\pi^+$ decays. This is expected to be the most promising method as it exploits the displaced B_c^+-vertex signature to suppress background; a similar approach has recently been demonstrated in a search for the $D^{*0} \to \mu^+\mu^-$ decay [16]. The inclusion of charge-conjugate processes is implied throughout the paper.

The analysis follows procedures from a recent search for nonresonant $B_c^+ \to \pi^+\mu^+\mu^-$ decays [17]. The results of that analysis include an upper limit on the ratio $\mathcal{B}(B_c^+ \to \pi^+\mu^+\mu^-)/\mathcal{B}(B_c^+ \to J/\psi\pi^+) < 1.9 \times 10^{-4}$ at 90% confidence level (CL) in the interval $15.0 < q^2 < 35.0\,\text{GeV}^2/c^4$, where $q^2 = m^2(\mu^+\mu^-)$ is the square of the invariant mass of the dimuon system. That result can be used to set limits on the branching fraction products $\mathcal{B}(B_c^+ \to B_s^{*0}\pi^+) \times \mathcal{B}(B_s^{*0} \to \mu^+\mu^-)$ and $\mathcal{B}(B_c^+ \to B^{*0}\pi^+) \times \mathcal{B}(B^{*0} \to \mu^+\mu^-)$, since such decays would contribute in the relevant q^2 region. However, due to the narrow $B_{(s)}^{*0}$ width, significantly better experimental sensitivity can be obtained by a dedicated search with optimised selection requirements and fit strategy, as presented here. The previous result also implies that the contribution from nonresonant $B_c^+ \to \pi^+\mu^+\mu^-$ decays is negligible, and therefore these decays do not need to be considered as a source of background in the data used for the $B_{(s)}^{*0}$ search.

To search for $B_c^+ \to B_{(s)}^{*0}(\mu^+\mu^-)\pi^+$ signals, the reconstructed B_c^+-candidate invariant mass, $m(\mu^+\mu^-\pi^+)$, and the dimuon invariant mass, $m(\mu^+\mu^-)$, serve as discriminating observables in an extended unbinned maximum-likelihood fit. The analysis uses the $B_c^+ \to J/\psi(\mu^+\mu^-)\,\pi^+$ decay as a normalisation mode. The signal yields, relative to that

for the normalisation mode, are translated into branching fraction ratios through

$$\begin{aligned}\mathcal{R}_{B^{*0}_{(s)}(\mu^+\mu^-)\pi^+/J/\psi\pi^+} &\equiv \frac{\mathcal{B}(B_c^+ \to B^{*0}_{(s)}(\mu^+\mu^-)\pi^+)}{\mathcal{B}(B_c^+ \to J/\psi\pi^+)} \\ &= \frac{N_{B^{*0}_{(s)}\pi^+}}{N_{J/\psi\pi^+}} \cdot \frac{\varepsilon_{J/\psi\pi^+}}{\varepsilon_{B^{*0}_{(s)}\pi^+}} \cdot \mathcal{B}(J/\psi \to \mu^+\mu^-) \\ &= \alpha^{\rm SES}_{B^{*0}_{(s)}\pi^+} \cdot N_{B^{*0}_{(s)}\pi^+}\,, \end{aligned} \tag{1}$$

where N denotes the yield of the mode indicated in the subscript, ε denotes the corresponding efficiency determined from simulation with data-driven corrections, and $\mathcal{B}(J/\psi \to \mu^+\mu^-)$ is the known branching fraction of the $J/\psi \to \mu^+\mu^-$ decay [18]. The single-event sensitivity $\alpha^{\rm SES}_{B^{*0}_{(s)}\pi^+}$ is the value of the ratio that would be obtained for one signal decay.

2 Detector and simulation

The LHCb detector [19, 20] is a single-arm forward spectrometer covering the pseudorapidity range $2 < \eta < 5$, designed for the study of particles containing b or c quarks. The detector includes a high-precision tracking system consisting of a silicon-strip vertex detector surrounding the pp interaction region [21], a large-area silicon-strip detector located upstream of a dipole magnet with a bending power of about 4 T m, and three stations of silicon-strip detectors and straw drift tubes [22, 23] placed downstream of the magnet. The tracking system provides a measurement of the momentum, p, of charged particles with a relative uncertainty that varies from 0.5% at low momentum to 1.0% at 200 GeV/c. The minimum distance of a track to a primary pp collision vertex (PV), the impact parameter (IP), is measured with a resolution of $(15 + 29/p_{\rm T})$ µm, where $p_{\rm T}$ is the component of the momentum transverse to the beam, in GeV/c. Different types of charged hadrons are distinguished using information from two ring-imaging Cherenkov detectors [24]. Photons, electrons and hadrons are identified by a calorimeter system consisting of scintillating-pad and preshower detectors, an electromagnetic and a hadronic calorimeter. Muons are identified by a system composed of alternating layers of iron and multiwire proportional chambers [25].

The online event selection is performed by a trigger [26, 27], which consists of a hardware stage, based on information from the calorimeter and muon systems, followed by a two-level software stage, which reconstructs the full event. Candidate $B_c^+ \to \pi^+\mu^+\mu^-$ decays are triggered as described in Ref. [16] for B^+ decays to the same final states. The hardware stage of the trigger selects events containing at least one muon with high $p_{\rm T}$. The following software stage selects events containing at least one high-$p_{\rm T}$ muon detached from any PV. The events must contain at least one secondary vertex (formed by two or more of the final-state particles) that is also detached from any PV. Secondary vertices consistent with the decay of a b hadron are identified by multivariate algorithms [28, 29].

Simulation is used to optimise the event selection procedure, to model the shape of invariant-mass distributions and to estimate efficiencies accounting for the effects of the detector acceptance, reconstruction and selection criteria. In the simulation, pp collisions are generated using Pythia [30] with a specific LHCb configuration [31]. The production of B_c^+ mesons is simulated using the dedicated generator BcVegPy [32]. Decays of unstable particles are described by EvtGen [33], in which final-state radiation is generated using

PHOTOS [34]. The interaction of the generated particles with the detector, and its response, are implemented using the GEANT4 toolkit [35–37].

The B_c^+ candidates reconstructed in simulation are weighted to correct for discrepancies between data and simulation associated with the particle-identification [38], track-reconstruction [39] and hardware-trigger [26] efficiencies. The simulation is also corrected such that the B_c^+ lifetime corresponds to the current experimental value [18, 40, 41]. Additional corrections are applied to account for discrepancies in B_c^+ production kinematics, event track multiplicity and other observables used in the selection of B_c^+ candidates. These corrections are obtained using a multivariate weighting algorithm [42], which is trained using $B_c^+ \to J/\psi\pi^+$ decays in background-subtracted data and simulation. After the corrections are applied, the simulated distributions of all variables used in the analysis are in good agreement with the data.

3 Candidate selection and background sources

The initial stages of the offline selection are identical to those for the recent search for nonresonant $B_c^+ \to \pi^+\mu^+\mu^-$ decays [17]. The B_c^+ candidates are formed from pairs of oppositely charged tracks identified as muons together with a track identified as a pion. The tracks are required to form a vertex with a good kinematic-fit quality that is displaced from every PV. Each B_c^+ candidate must have a momentum vector that is aligned with the direction between one of the PVs, subsequently referred to as the associated PV, and the B_c^+-candidate decay vertex.

Each B_c^+ candidate is required to have an invariant mass in the range $6150 < m(\pi^+\mu^+\mu^-) < 6700\,\text{MeV}/c^2$. The expected signal resolution in $m(\pi^+\mu^+\mu^-)$ is about $20\,\text{MeV}/c^2$. The dimuon invariant mass is calculated from the outcome of a kinematic fit in which the B_c^+-candidate invariant mass is constrained to the known B_c^+ mass [18] and the momentum vector is constrained to be consistent with the line of flight between the associated PV and the decay vertex, thereby improving the resolution. The dimuon invariant mass is required to be in the range $5225 < m(\mu^+\mu^-) < 5515\,\text{MeV}/c^2$ for the signal modes and $3000 < m(\mu^+\mu^-) < 3200\,\text{MeV}/c^2$ for the normalisation mode. The expected signal resolution in $m(\mu^+\mu^-)$ is about $4\,\text{MeV}/c^2$.

Combinatorial background arising from random combinations of tracks is suppressed using a boosted decision tree (BDT) classifier [43, 44] that has been trained and validated to identify $B_c^+ \to \pi^+\mu^+\mu^-$ signal candidates, such that its performance is independent of the dimuon invariant mass [17]. The BDT classifier receives as inputs the p_{T} of the pion track, the highest p_{T} among muon tracks, the IPs of the muon tracks and of the B_c^+ candidate with respect to the associated PV, the B_c^+ flight distance, the vertex quality of the B_c^+ candidate, and the largest distance of closest approach between any two of the final-state particles.

Further suppression of combinatorial background is obtained by applying a requirement on the cosine of the helicity angle θ_l, which is defined as the angle between the μ^+ direction and the direction opposite of the B_c^+ momentum in the dimuon rest frame. This has additional discrimination power since the signal and normalisation modes follow a $1-\cos^2\theta_l$ distribution while the combinatorial background sharply peaks at $\cos\theta_l \approx \pm 1$.

Requirements on the BDT classifier output, the absolute value of $\cos\theta_l$, and variables characterising the charged-pion particle identification are optimised simultaneously.

The optimisation is based on a grid search to obtain the best signal sensitivity using the figure of merit $\varepsilon/(5/2+\sqrt{N_{\rm B}})$ [45], where ε is the signal efficiency and $N_{\rm B}$ is the expected number of background candidates in the signal region. The figure of merit is evaluated separately for $B_c^+ \to B^{*0}(\mu^+\mu^-)\pi^+$ and $B_c^+ \to B_s^{*0}(\mu^+\mu^-)\pi^+$ decays. The signal region for each decay mode corresponds to a two-dimensional range in $m(\pi^+\mu^+\mu^-)$ and $m(\mu^+\mu^-)$ of about ± 3 times the expected resolution in each dimension, centred at the expected two-dimensional peak position [18]. The expected background yield is estimated by fitting a background-only model to the dataset excluding the region $6215 < m(\pi^+\mu^+\mu^-) < 6335\,{\rm MeV}/c^2$.

The figures of merit for both $B_c^+ \to B^{*0}(\mu^+\mu^-)\pi^+$ and $B_c^+ \to B_s^{*0}(\mu^+\mu^-)\pi^+$ decays have maximum values at the same grid point. With the optimised requirements, the classifier has a combinatorial background rejection power of 99%, whilst retaining 65% of signal decays. The optimised angular selection, corresponding to $|\cos\theta_l| < 0.90$, further rejects about 30% of the combinatorial background, whilst keeping about 98% of signal decays. The particle-identification requirements have a pion efficiency around 90%, with a kaon misidentification rate around 10%. The particle-identification requirements applied to the muon candidates have an efficiency around 99%, with a pion misidentification rate below 1%. The same selection requirements are used for signal and normalisation modes to reduce potential systematic biases on the measurement of branching fraction ratios. After applying the selection requirements, each selected event contains only one B_c^+ candidate.

Backgrounds from partially reconstructed decays, such as $B_c^+ \to J/\psi\rho^+(\pi^+\pi^0)$ [46] for the normalisation mode, have a reconstructed B_c^+-candidate invariant mass that lies more than $100\,{\rm MeV}/c^2$ below the known B_c^+ mass [18]. These sources of background predominantly populate a region outside, but have a tail that extends into, the fit range used in the analysis. This is also the case for backgrounds such as $B_c^+ \to \rho^+\mu^+\mu^-$ for the signal modes, but these were found to be negligible in the search for nonresonant $B_c^+ \to \pi^+\mu^+\mu^-$ decays [17]. The partially reconstructed background contribution is therefore neglected in the fit for the signal modes, but is accounted for in the normalisation mode fit. Processes with a missing neutrino or two or more missing massive particles can also be a source of partially reconstructed background, but their contributions are negligible in the fit range.

Contributions from hadronic backgrounds such as $B_c^+ \to \pi^+\pi^-\pi^+$ decays, where two pions are mistakenly identified as muons, were found to be negligible in the search for nonresonant $B_c^+ \to \pi^+\mu^+\mu^-$ decays [17] and are therefore neglected. Similarly, possible contributions from the resonant $B_c^+ \to J/\psi\pi^+$ or $B_c^+ \to \psi(2S)\pi^+$ decays, where the pion is mistakenly identified as one of the two muons and vice versa, were studied using simulation and data and found to be negligible after applying the selection requirements. Contributions from $B_c^+ \to B_{(s)}^0\pi^+ \to \mu^+\mu^-\pi^+$ decays are negligible due to their small rates [9–12] and due to the selection requirements, which suppress topologies with a $\mu^+\mu^-$ vertex displaced from the B_c^+-decay vertex.

For the normalisation mode, misidentified background can arise from the $B_c^+ \to J/\psi K^+$ mode. The branching fraction for this decay is Cabibbo-suppressed with respect to that for the $B_c^+ \to J/\psi\pi^+$ decay, and their ratio has been measured to be $0.079 \pm 0.007 \pm 0.003$ [47]. This background is further suppressed by the particle-identification requirements, but nonetheless is accounted for in the normalisation mode fit.

4 Invariant-mass fits

The yield of the $B_c^+ \to J/\psi(\mu^+\mu^-)\,\pi^+$ normalisation mode is determined from a one-dimensional extended unbinned maximum-likelihood fit to the $m(\pi^+\mu^+\mu^-)$ distribution of candidates in the range $3000 < m(\mu^+\mu^-) < 3200\,\text{MeV}/c^2$. The normalisation mode also provides correction factors that account for discrepancies between data and simulation in the signal peak positions and widths. The relevant factors for the dimuon signal shape are obtained from an additional maximum-likelihood fit to the $m(\mu^+\mu^-)$ distribution. The B_c^+-candidate invariant-mass and dimuon invariant-mass fits to the normalisation mode are independent of each other. A two-dimensional fit is avoided since possible correlations in the tail regions of the two observables could result in a non-negligible fit bias given the large sample size.

For the B_c^+-candidate invariant-mass fit for the normalisation mode, the fit model includes four components: signal $B_c^+ \to J/\psi\pi^+$ decays, misidentified $B_c^+ \to J/\psi K^+$ decays, partially reconstructed background from $B_c^+ \to J/\psi\rho^+$ decays and combinatorial background. The signal, misidentified and partially reconstructed backgrounds are each modelled by the sum of two Gaussian functions, one of which has power-law tails [48]. The relative fraction between the two Gaussian functions and the tail parameters of each distribution are fixed from simulation. The peak position and width of the distributions are allowed to vary in the fit to the data by a global shift and scaling factor, respectively, that are shared between these three components. The combinatorial background model is an exponential function with a slope that is allowed to vary. In total, the fit includes seven parameters: the yields of the four components, the global peak position shift and width scaling factor, and the slope of the combinatorial background. The yield for misidentified $B_c^+ \to J/\psi K^+$ decays is allowed to vary with respect to the yield for the $B_c^+ \to J/\psi\pi^+$ decays within a Gaussian constraint based on the expected misidentification rate [38] and the measured branching fraction ratio [47].

For the dimuon invariant-mass fit, the fit model includes a signal and a combinatorial background component. The signal is modelled by a Gaussian function with power-law tails, while the background is modelled by a first-order polynomial function. The tail parameters of the signal model are fixed from $B_c^+ \to J/\psi\pi^+$ simulation. The signal peak position and width are allowed to vary in the fit to the data through a shift and a width scaling factor. The fit to the dimuon-mass includes five free parameters: the yields for the two components, the shift of peak position and width scaling factor, and the slope of the combinatorial background.

Figure 1 shows the dimuon and B_c^+-candidate invariant-mass distributions of selected $B_c^+ \to J/\psi\pi^+$ candidates. The B_c^+-candidate invariant-mass fit converges to a yield of 6213 ± 89 decays, where the uncertainty is statistical only.

The dimuon invariant-mass distribution in data can receive contributions from J/ψ decays that do not stem from the $B_c^+ \to J/\psi\pi^+$ process. This background contribution could affect the fit results for the shift and width scaling factors. To check this and also the effect of dependencies in the tails between B_c^+-mass and dimuon mass distributions, the fit is repeated restricting the B_c^+-candidates to the region $6215 < m(\pi^+\mu^+\mu^-) < 6335\,\text{MeV}/c^2$. The results for the shift and width scaling factor obtained from this fit demonstrate that the values obtained from the nominal fit are robust against systematic variations.

The signal $B_c^+ \to B^{*0}(\mu^+\mu^-)\pi^+$ and $B_c^+ \to B_s^{*0}(\mu^+\mu^-)\pi^+$ yields are determined from a two-dimensional extended unbinned maximum-likelihood fit to the $m(\mu^+\mu^-)$

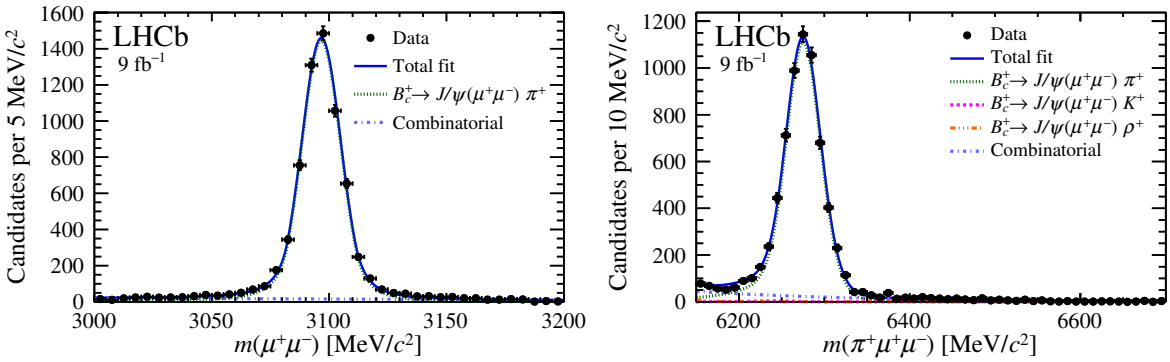

Figure 1: Reconstructed (left) $\mu^+\mu^-$ and (right) $\pi^+\mu^+\mu^-$ invariant-mass distributions for the selected $B_c^+ \to J/\psi(\mu^+\mu^-)\pi^+$ candidates, with results of the fit superimposed. The distributions are dominated by signal, and the background contributions are barely visible.

and $m(\pi^+\mu^+\mu^-)$ distributions. The fit model includes three components: signal $B_c^+ \to B^{*0}(\mu^+\mu^-)\pi^+$ decays, signal $B_c^+ \to B_s^{*0}(\mu^+\mu^-)\pi^+$ decays and combinatorial background. For each component, the total model is the product of the respective dimuon and B_c^+-candidate invariant-mass models. The models for the signal components are validated using simulation. The two fit observables are found to not be significantly correlated in simulation or sideband data and are therefore treated as uncorrelated.

For the signal components, the dimuon and the B_c^+-candidate invariant-mass distributions are each modelled using a Gaussian function with power-law tails on both sides of the peak. The tail parameters are fixed to the values obtained from simulation. The signal dimuon and B_c^+-candidate invariant-mass models each include a global shift of peak position and a global scaling factor for the width of the distribution, relative to the values found in simulation. For the combinatorial background, the dimuon and the B_c^+-candidate invariant-mass distributions are modelled using a linear function and an exponential function, respectively, with slope parameters allowed to vary in the fit to data.

In total, the fit includes five free parameters: the yields for each component and the two parameters of the combinatorial background model. In addition, the global peak position shift and width scaling factor for each of the dimuon and B_c^+-candidate invariant-mass models are allowed to vary within Gaussian constraints based on the values obtained from the fits for the $B_c^+ \to J/\psi(\mu^+\mu^-)\,\pi^+$ candidates.

Figure 2 shows the dimuon and B_c^+-candidate invariant-mass distributions of selected $B_c^+ \to B_{(s)}^{*0}(\mu^+\mu^-)\pi^+$ candidates, with results of the fit superimposed. Figure 3 shows the two-dimensional distribution of selected candidates together with the one-dimensional distributions of dimuon invariant-mass in the range $6215 < m(\pi^+\mu^+\mu^-) < 6335\,\text{MeV}/c^2$ and $\pi^+\mu^+\mu^-$ invariant-mass in the ranges $5313 < m(\mu^+\mu^-) < 5337\,\text{MeV}/c^2$ and $5404 < m(\mu^+\mu^-) < 5428\,\text{MeV}/c^2$. These signal-enhanced, one-dimensional distributions are shown with the results of the fit superimposed. The yields for the $B_c^+ \to B^{*0}(\mu^+\mu^-)\pi^+$ and $B_c^+ \to B_s^{*0}(\mu^+\mu^-)\pi^+$ decays are consistent with zero. Table 1 summarises the yields obtained from the fit. The fit returns a correlation between the two signal yields of 1.2%.

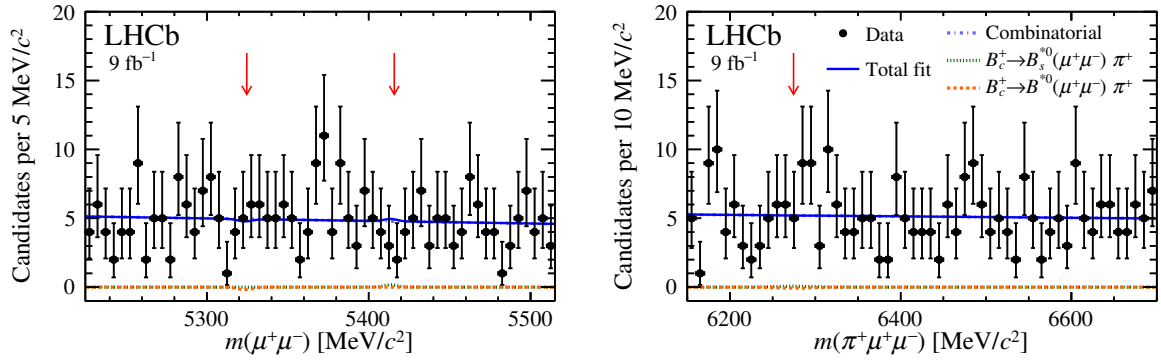

Figure 2: Reconstructed (left) $\mu^+\mu^-$ and (right) $\pi^+\mu^+\mu^-$ invariant-mass distributions for the selected $B_c^+ \to B_{(s)}^{*0}(\mu^+\mu^-)\pi^+$ candidates, with results of the fit superimposed. The red arrows point to the expected signal peak positions. The signal yields are consistent with zero and therefore the $B_c^+ \to B^{*0}(\mu^+\mu^-)\pi^+$ and $B_c^+ \to B_s^{*0}(\mu^+\mu^-)\pi^+$ components are barely visible.

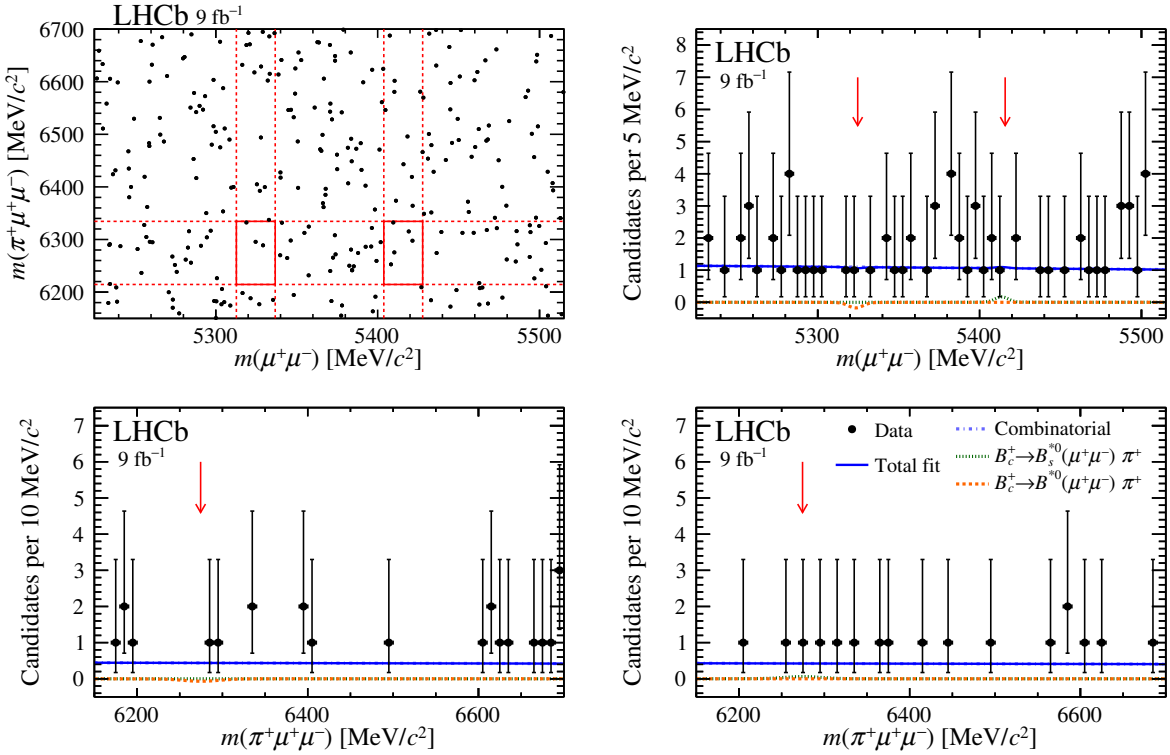

Figure 3: The (top left) two-dimensional distribution of $\pi^+\mu^+\mu^-$ invariant mass versus $\mu^+\mu^-$ invariant mass for the selected $B_c^+ \to B_{(s)}^{*0}(\mu^+\mu^-)\pi^+$ candidates, together with the (top right) $\mu^+\mu^-$ invariant-mass distribution in the range $6215 < m(\pi^+\mu^+\mu^-) < 6335\,\text{MeV}/c^2$ and the $\pi^+\mu^+\mu^-$ invariant-mass distributions in the ranges (bottom left) $5313 < m(\mu^+\mu^-) < 5337\,\text{MeV}/c^2$ and (bottom right) $5404 < m(\mu^+\mu^-) < 5428\,\text{MeV}/c^2$, with results of the fit superimposed. The areas delimited by the full red lines in the top left figure show the intersections of the aforementioned ranges, which correspond to about ± 3 times the experimental resolution around the expected signal-peak positions in each dimension. The red arrows point to the expected signal peak positions. The signal yields are consistent with zero and therefore the $B_c^+ \to B^{*0}(\mu^+\mu^-)\pi^+$ and $B_c^+ \to B_s^{*0}(\mu^+\mu^-)\pi^+$ components are barely visible.

Table 1: Yields obtained from the fit to data described in the text, with statistical uncertainties only.

Component	Yield
$B_c^+ \to B^{*0}(\mu^+\mu^-)\pi^+$	$-0.4\,^{+1.9}_{-1.1}$
$B_c^+ \to B_s^{*0}(\mu^+\mu^-)\pi^+$	$0.4\,^{+2.2}_{-1.3}$
Combinatorial background	282 ± 17

5 Efficiencies and systematic uncertainties

Table 2 summarises the parameters entering the determination of the single-event sensitivities in Eq. (1), with statistical and systematic uncertainties added in quadrature. Systematic uncertainties on the signal yields are not included in this procedure, but are instead studied as a cross-check of the procedure and are found to be negligible.

The efficiency ratios between signal and normalisation modes are obtained from simulation accounting for the geometrical acceptance of the detector as well as effects related to the triggering, reconstruction and selection of the B_c^+ candidates. The uncertainties on the efficiency ratios take into account the simulation sample size, uncertainties on the weights applied to the simulation, the matching between reconstructed and generated particles in the simulation, variations of the software trigger requirements, and the uncertainty on the known B_c^+ lifetime. All variations are made consistently for the signal and normalisation modes to avoid overestimation of the uncertainty on the efficiency ratio.

The systematic uncertainties associated with the weights are evaluated by varying all weights within their statistical uncertainties and by varying the binning scheme used to estimate them. The systematic uncertainty associated with the multivariate weighting algorithm (see Sec. 2) is evaluated by comparing the results obtained with the default and with an alternative algorithm. The default algorithm is trained to correct for discrepancies between data and simulation associated with the event track multiplicity and with the transverse momentum and the vertex quality of the B_c^+ candidates. The alternative algorithm is trained using the impact parameter significance of the two muons as additional inputs.

The systematic uncertainty associated with the matching between reconstructed and generated particles in the simulation is evaluated by comparing the efficiencies obtained

Table 2: Input parameters used in the estimation of the ratio $\mathcal{R}_{B_{(s)}^{*0}(\mu^+\mu^-)\pi^+/J/\psi\pi^+}$. The $J/\psi \to \mu^+\mu^-$ branching fraction and its uncertainty are taken from Ref. [18]. For the $B_c^+ \to J/\psi\pi^+$ yield the uncertainties are statistical and systematic, respectively; all other uncertainties are systematic.

Parameter	Value
$\mathcal{B}(J/\psi \to \mu^+\mu^-)$	$(59.61 \pm 0.33) \times 10^{-3}$
$N_{J/\psi\pi^+}$	$6213 \pm 89 \pm 27$
$\varepsilon_{J/\psi\pi^+}/\varepsilon_{B^{*0}\pi^+}$	1.09 ± 0.05
$\varepsilon_{J/\psi\pi^+}/\varepsilon_{B_s^{*0}\pi^+}$	1.18 ± 0.05

including or excluding B candidates for which one or more decay products are not correctly matched. The systematic uncertainty associated with variations of the software trigger requirements that are not reproduced by the simulation is evaluated by comparing the efficiencies obtained by applying the tightest thresholds and by applying average thresholds within each data-taking period. The systematic uncertainty associated with the B_c^+ lifetime is evaluated by varying the B_c^+ lifetime in simulation within its uncertainties [18].

A further systematic effect associated with the track reconstruction [39] can arise due to the possible difference in hadronic interactions for the pion tracks in the signal and the normalisation modes (due to the kinematic differences between the decays) and discrepancies between data and simulation in the detector material. This effect is studied in simulation and data and is found to have a negligible impact.

The effect of the multivariate weighting algorithm has the largest impact on the systematic uncertainty of the efficiency ratio. The remaining systematic uncertainties cancel out almost completely in the determination of the efficiency ratios and are smaller than the statistical uncertainties.

The normalisation mode yield obtained in the previous section can be affected by the fit model choice and by the assumption of the polarisation of the partially reconstructed backgrounds. To study the effect of the fit model choice, each fit is performed in three configurations: using the baseline fit model and using two alternative fit models. In the two alternative fit models, the analytical function used for the combinatorial background is replaced by a sigmoid function. In the first alternative model the same parametrisation as in the nominal model is kept for the other fit components, while in the second alternative model the $B_c^+ \to J/\psi\pi^+$ and the misidentified background models are replaced by a modified hyperbolic distribution with power-law tails [49] and the model for the partially reconstructed background is replaced by a Gaussian function with a power-law tail to the right side of the distribution. For the normalisation mode yield, the largest difference between the results obtained with the baseline and alternative models is assigned as systematic uncertainty. For the global peak shift and width scaling factors, the model choice is found to have a negligible impact.

In the nominal normalisation mode fit, the ρ^+ meson in the $B_c^+ \to J/\psi\rho^+$ partially reconstructed background is assumed to be unpolarised. However, the polarisation of the ρ^+ meson can affect the momentum of the missing pion and hence the B_c^+-candidate mass shape of the partially reconstructed backgrounds. The fit is therefore repeated assuming either full longitudinal or full transverse ρ^+ polarisation. The difference in the results for the two configurations is found to be negligible.

6 Results for relative branching fractions

The fit is repeated with a model identical to that described in Sec. 4, except that the signal yields are parametrised in terms of branching fraction ratios $\mathcal{R}_{B^{*0}_{(s)}(\mu^+\mu^-)\pi^+/J/\psi\pi^+}$ using Eq. (1). The systematic uncertainties associated with the single-event sensitivities are accounted for through Gaussian constraints in the fit. Using the parameters in Table 2 to calculate the single-event sensitivities gives $\alpha^{\rm SES}_{B^{*0}\pi^+} = (1.04 \pm 0.05) \times 10^{-5}$ and $\alpha^{\rm SES}_{B^{*0}_s\pi^+} = (1.13 \pm 0.05) \times 10^{-5}$ taking statistical and systematic uncertainties into account.

Including all constraints, the fit yields

$$\mathcal{R}_{B^{*0}(\mu^+\mu^-)\pi^+/J/\psi\pi^+} = (-0.44\,^{+1.99}_{-1.12}) \times 10^{-5}\,,$$
$$\mathcal{R}_{B_s^{*0}(\mu^+\mu^-)\pi^+/J/\psi\pi^+} = \quad (0.43\,^{+2.45}_{-1.41}) \times 10^{-5}\,.$$

To assess the impact of the systematic uncertainties, the fits are repeated fixing the nuisance parameters to their central values. The difference in the uncertainties between the two configurations is around 10^{-7}, showing that the impact of the systematic uncertainties is negligible.

Upper limits on the branching fraction ratios are obtained following the Feldman–Cousins prescription [50]: pseudoexperiments are generated for various values of $\mathcal{R}_{B^{*0}_{(s)}(\mu^+\mu^-)\pi^+/J/\psi\pi^+}$ and the distributions of the measured $\mathcal{R}_{B^{*0}_{(s)}(\mu^+\mu^-)\pi^+/J/\psi\pi^+}$ values in the pseudoexperiments are used to form confidence belts. Nuisance parameters are varied within their uncertainties in the generation of the pseudoexperiments. The scan to obtain limits for $\mathcal{R}_{B^{*0}(\mu^+\mu^-)\pi^+/J/\psi\pi^+}$ is performed assuming that $\mathcal{R}_{B_s^{*0}(\mu^+\mu^-)\pi^+/J/\psi\pi^+}$ is zero and vice versa. This assumption does not impact the obtained limits as the correlation between the signal yields is negligible. Figure 4 shows confidence belts at 90% and 95% CL. Evaluation of the upper limits at the central values obtained from the fit to data yields

$$\mathcal{R}_{B^{*0}(\mu^+\mu^-)\pi^+/J/\psi\pi^+} < 3.8\,(5.2) \times 10^{-5} \text{ at } 90\ (95)\%\,\text{CL}\,,$$
$$\mathcal{R}_{B_s^{*0}(\mu^+\mu^-)\pi^+/J/\psi\pi^+} < 5.0\,(6.3) \times 10^{-5} \text{ at } 90\ (95)\%\,\text{CL}\,.$$

As further checks, the procedure is repeated restricting the signal yield to positive values, or replacing in the fit model the signal parametrisation with the sum of two Gaussian functions, one with power-law tails. No significant changes in the obtained upper limits are found.

As a further cross-check, the ratio $\mathcal{B}(B_c^+ \to \psi(2S)(\mu^+\mu^-)\pi^+)/\mathcal{B}(B_c^+ \to J/\psi(\mu^+\mu^-)\pi^+)$ is measured following the same analysis procedure as in Ref. [17], but applying the BDT classifier, $\cos\theta_l$ and particle-identification requirements optimised for this work. The measured value is 0.279 ± 0.025, where the uncertainty is statistical only. This is consistent within 1.5 standard deviations with the results in Ref. [17] when accounting for correlations, and it also agrees with previously published measurements of this quantity [51, 52].

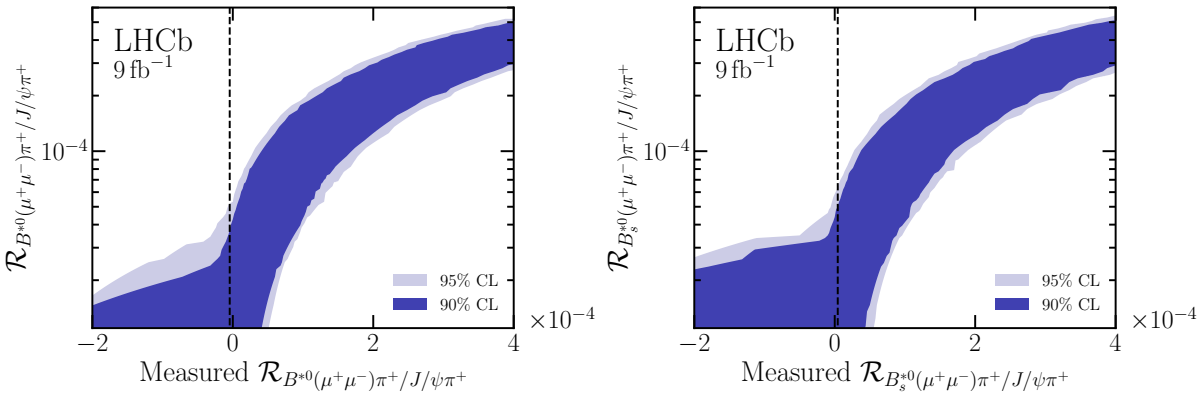

Figure 4: Confidence belts generated using pseudoexperiments according to the Feldman–Cousins prescription. The vertical black line shows the results of the fit to data.

7 Summary

A search is performed for the very rare $B^{*0} \to \mu^+\mu^-$ and $B_s^{*0} \to \mu^+\mu^-$ decays by analysing $B_c^+ \to \pi^+\mu^+\mu^-$ decays. The analysis uses proton-proton collision data collected with the LHCb detector between 2011 and 2018, corresponding to an integrated luminosity of $9\,\text{fb}^{-1}$. No evidence for an excess of signal events over background is observed for the two decay modes and the first upper limits on their branching fraction ratios are obtained,

$$\mathcal{R}_{B^{*0}(\mu^+\mu^-)\pi^+/J/\psi\pi^+} < 3.8 \times 10^{-5}\,,$$
$$\mathcal{R}_{B_s^{*0}(\mu^+\mu^-)\pi^+/J/\psi\pi^+} < 5.0 \times 10^{-5}\,,$$

at 90% confidence level. Once measurements of the ratio $\mathcal{B}(B_c^+ \to B_{(s)}^{*0}\pi^+)/\mathcal{B}(B_c^+ \to J/\psi\pi^+)$ become available, it will be possible to translate these results into limits on the absolute $B_{(s)}^{*0} \to \mu^+\mu^-$ branching fractions.

Acknowledgements

We express our gratitude to our colleagues in the CERN accelerator departments for the excellent performance of the LHC. We thank the technical and administrative staff at the LHCb institutes. We acknowledge support from CERN and from the national agencies: CAPES, CNPq, FAPERJ and FINEP (Brazil); MOST and NSFC (China); CNRS/IN2P3 (France); BMBF, DFG and MPG (Germany); INFN (Italy); NWO (Netherlands); MNiSW and NCN (Poland); MCID/IFA (Romania); MICIU and AEI (Spain); SNSF and SER (Switzerland); NASU (Ukraine); STFC (United Kingdom); DOE NP and NSF (USA). We acknowledge the computing resources that are provided by CERN, IN2P3 (France), KIT and DESY (Germany), INFN (Italy), SURF (Netherlands), PIC (Spain), GridPP (United Kingdom), CSCS (Switzerland), IFIN-HH (Romania), CBPF (Brazil), and Polish WLCG (Poland). We are indebted to the communities behind the multiple open-source software packages on which we depend. Individual groups or members have received support from ARC and ARDC (Australia); Key Research Program of Frontier Sciences of CAS, CAS PIFI, CAS CCEPP, Fundamental Research Funds for the Central Universities, and Sci. & Tech. Program of Guangzhou (China); Minciencias (Colombia); EPLANET, Marie Skłodowska-Curie Actions, ERC and NextGenerationEU (European Union); A*MIDEX, ANR, IPhU and Labex P2IO, and Région Auvergne-Rhône-Alpes (France); AvH Foundation (Germany); ICSC (Italy); Severo Ochoa and María de Maeztu Units of Excellence, GVA, XuntaGal, GENCAT, InTalent-Inditex and Prog. Atracción Talento CM (Spain); SRC (Sweden); the Leverhulme Trust, the Royal Society and UKRI (United Kingdom).

References

[1] G. Buchalla, A. J. Buras, and M. E. Lautenbacher, *Weak decays beyond leading logarithms*, Rev. Mod. Phys. **68** (1996) 1125, arXiv:hep-ph/9512380.

[2] B. Grinstein and J. Martin Camalich, *Weak decays of excited B mesons*, Phys. Rev. Lett. **116** (2016) 141801, arXiv:1509.05049.

[3] A. Khodjamirian, T. Mannel, and A. A. Petrov, *Direct probes of flavor-changing neutral currents in e^+e^- collisions*, JHEP **11** (2015) 142, arXiv:1509.07123.

[4] G.-Z. Xu, Y. Qiu, C.-P. Shen, and Y.-J. Zhang, *$B^*_{s,d} \to \mu^+\mu^-$ and its impact on $B_{s,d} \to \mu^+\mu^-$*, Eur. Phys. J. **C76** (2016) 583, arXiv:1601.03386.

[5] S. Sahoo and R. Mohanta, *Study of the rare decays $B^*_{s,d} \to \mu^+\mu^-$*, J. Phys. **G44** (2017) 035001, arXiv:1612.02543.

[6] D. Banerjee, P. Maji, and S. Sahoo, *Study of the rare decays $B^*_{s,d} \to l^+l^-$ in Z' model*, Int. J. Mod. Phys. **A32** (2017) 1750075, arXiv:1712.05544.

[7] D. Kumar, J. Saini, S. Gangal, and S. B. Das, *Probing new physics through $B^*_s \to \mu^+\mu^-$ decay*, Phys. Rev. **D97** (2018) 035007, arXiv:1711.01989.

[8] S. Kumbhakar and J. Saini, *New physics effects in purely leptonic B^*_s decays*, Eur. Phys. J. **C79** (2019) 394, arXiv:1807.04055.

[9] LHCb collaboration, R. Aaij *et al.*, *Analysis of neutral B-meson decays into two muons*, Phys. Rev. Lett. **128** (2022) 041801, arXiv:2108.09284.

[10] LHCb collaboration, R. Aaij *et al.*, *Measurement of the $B^0_s \to \mu^+\mu^-$ decay properties and search for the $B^0 \to \mu^+\mu^-$ and $B^0_s \to \mu^+\mu^-\gamma$ decays*, Phys. Rev. **D105** (2022) 012010, arXiv:2108.09283.

[11] CMS collaboration, A. Tumasyan *et al.*, *Measurement of the $B^0_s \to \mu^+\mu^-$ decay properties and search for the $B^0 \to \mu^+\mu^-$ decay in proton-proton collisions at $\sqrt{s} = 13$ TeV*, Phys. Lett. **B842** (2023) 137955, arXiv:2212.10311.

[12] ATLAS collaboration, M. Aaboud *et al.*, *Study of the rare decays of B^0_s and B^0 mesons into muon pairs using data collected during 2015 and 2016 with the ATLAS detector*, JHEP **04** (2019) 098, arXiv:1812.03017.

[13] LHCb collaboration, R. Aaij *et al.*, *Search for the rare decays $B^0_s \to e^+e^-$ and $B^0 \to e^+e^-$*, Phys. Rev. Lett. **124** (2020) 211802, arXiv:2003.03999.

[14] LHCb collaboration, R. Aaij *et al.*, *Search for the decays $B^0_s \to \tau^+\tau^-$ and $B^0 \to \tau^+\tau^-$*, Phys. Rev. Lett. **118** (2017) 251802, arXiv:1703.02508.

[15] F. Abudinén, T. Blake, U. Egede, and T. Gershon, *Prospects for studies of $D^{*0} \to \mu^+\mu^-$ and $B^{*0}_{(s)} \to \mu^+\mu^-$ decays*, Eur. Phys. J. **C82** (2022) 459, arXiv:2202.03916.

[16] LHCb collaboration, R. Aaij *et al.*, *Search for $D^*(2007)^0 \to \mu^+\mu^-$ in $B^- \to \pi^-\mu^+\mu^-$ decays*, Eur. Phys. J. **C83** (2023) 666, arXiv:2304.01981.

[17] LHCb collaboration, R. Aaij *et al.*, *Search for $B^+_c \to \pi^+\mu^+\mu^-$ decays and measurement of the branching fraction ratio $\mathcal{B}(B^+_c \to \psi(2S)\pi^+)/\mathcal{B}(B^+_c \to J/\psi\pi^+)$*, Eur. Phys. J. **C84** (2024) 468, arXiv:2312.12228.

[18] Particle Data Group, S. Navas *et al.*, *Review of particle physics*, Phys. Rev. **D110** (2024) 030001.

[19] LHCb collaboration, A. A. Alves Jr. *et al.*, *The LHCb detector at the LHC*, JINST **3** (2008) S08005.

[20] LHCb collaboration, R. Aaij *et al.*, *LHCb detector performance*, Int. J. Mod. Phys. **A30** (2015) 1530022, arXiv:1412.6352.

[21] R. Aaij *et al.*, *Performance of the LHCb Vertex Locator*, JINST **9** (2014) P09007, arXiv:1405.7808.

[22] R. Arink *et al.*, *Performance of the LHCb Outer Tracker*, JINST **9** (2014) P01002, arXiv:1311.3893.

[23] P. d'Argent *et al.*, *Improved performance of the LHCb Outer Tracker in LHC Run 2*, JINST **12** (2017) P11016, arXiv:1708.00819.

[24] M. Adinolfi *et al.*, *Performance of the LHCb RICH detector at the LHC*, Eur. Phys. J. **C73** (2013) 2431, arXiv:1211.6759.

[25] A. A. Alves Jr. *et al.*, *Performance of the LHCb muon system*, JINST **8** (2013) P02022, arXiv:1211.1346.

[26] R. Aaij *et al.*, *The LHCb trigger and its performance in 2011*, JINST **8** (2013) P04022, arXiv:1211.3055.

[27] R. Aaij *et al.*, *Design and performance of the LHCb trigger and full real-time reconstruction in Run 2 of the LHC*, JINST **14** (2019) P04013, arXiv:1812.10790.

[28] V. V. Gligorov and M. Williams, *Efficient, reliable and fast high-level triggering using a bonsai boosted decision tree*, JINST **8** (2013) P02013, arXiv:1210.6861.

[29] T. Likhomanenko *et al.*, *LHCb topological trigger reoptimization*, J. Phys. Conf. Ser. **664** (2015) 082025, arXiv:1510.00572.

[30] T. Sjöstrand, S. Mrenna, and P. Skands, *A brief introduction to PYTHIA 8.1*, Comput. Phys. Commun. **178** (2008) 852, arXiv:0710.3820.

[31] I. Belyaev *et al.*, *Handling of the generation of primary events in Gauss, the LHCb simulation framework*, J. Phys. Conf. Ser. **331** (2011) 032047.

[32] C.-H. Chang, J.-X. Wang, and X.-G. Wu, *BCVEGPY2.0: An upgraded version of the generator BCVEGPY with the addition of hadroproduction of the P-wave B_c^+ states*, Comput. Phys. Commun. **174** (2006) 241, arXiv:hep-ph/0504017.

[33] D. J. Lange, *The EvtGen particle decay simulation package*, Nucl. Instrum. Meth. **A462** (2001) 152.

[34] N. Davidson, T. Przedzinski, and Z. Was, *PHOTOS interface in C++: Technical and physics documentation*, Comp. Phys. Comm. **199** (2016) 86, arXiv:1011.0937.

[35] Geant4 collaboration, J. Allison *et al.*, *Geant4 developments and applications*, IEEE Trans. Nucl. Sci. **53** (2006) 270; Geant4 collaboration, S. Agostinelli *et al.*, *Geant4: A simulation toolkit*, Nucl. Instrum. Meth. **A506** (2003) 250.

[36] M. Clemencic *et al.*, *The LHCb simulation application, Gauss: Design, evolution and experience*, J. Phys. Conf. Ser. **331** (2011) 032023.

[37] D. Müller, M. Clemencic, G. Corti, and M. Gersabeck, *ReDecay: A novel approach to speed up the simulation at LHCb*, Eur. Phys. J. **C78** (2018) 1009, arXiv:1810.10362.

[38] R. Aaij *et al.*, *Selection and processing of calibration samples to measure the particle identification performance of the LHCb experiment in Run 2*, Eur. Phys. J. Tech. Instr. **6** (2019) 1, arXiv:1803.00824.

[39] LHCb collaboration, R. Aaij *et al.*, *Measurement of the track reconstruction efficiency at LHCb*, JINST **10** (2015) P02007, arXiv:1408.1251.

[40] LHCb collaboration, R. Aaij *et al.*, *Measurement of the B_c^+ meson lifetime using $B_c^+ \to J/\psi\mu^+\nu_\mu X$ decays*, Eur. Phys. J. **C74** (2014) 2839, arXiv:1401.6932.

[41] LHCb collaboration, R. Aaij *et al.*, *Measurement of the lifetime of the B_c^+ meson using the $B_c^+ \to J/\psi\pi^+$ decay mode*, Phys. Lett. **B742** (2015) 29, arXiv:1411.6899.

[42] A. Rogozhnikov, *Reweighting with boosted decision trees*, J. Phys. Conf. Ser. **762** (2016) 012036, arXiv:1608.05806, https://github.com/arogozhnikov/hep_ml.

[43] L. Breiman, J. H. Friedman, R. A. Olshen, and C. J. Stone, *Classification and regression trees*, Wadsworth international group, Belmont, California, USA, 1984.

[44] T. Chen and C. Guestrin, *XGBoost: A scalable tree boosting system*, in *Proceedings of the 22nd ACM SIGKDD International Conference on Knowledge Discovery and Data Mining*, KDD '16, (New York, NY, USA), 785–794, ACM, 2016.

[45] G. Punzi, *Sensitivity of searches for new signals and its optimization*, eConf **C030908** (2003) MODT002, arXiv:physics/0308063.

[46] LHCb collaboration, R. Aaij *et al.*, *Observation of the $B_c^+ \to J/\psi\pi^+\pi^0$ decay*, JHEP **02** (2024) 151, arXiv:2402.05523.

[47] LHCb collaboration, R. Aaij *et al.*, *Measurement of the ratio of branching fractions $\mathcal{B}(B_c^+ \to J/\psi K^+)/\mathcal{B}(B_c^+ \to J/\psi\pi^+)$*, JHEP **09** (2016) 153, arXiv:1607.06823.

[48] T. Skwarnicki, *A study of the radiative cascade transitions between the Upsilon-prime and Upsilon resonances*, PhD thesis, Institute of Nuclear Physics, Krakow, 1986, DESY-F31-86-02.

[49] D. Martínez Santos and F. Dupertuis, *Mass distributions marginalized over per-event errors*, Nucl. Instrum. Meth. **A764** (2014) 150, arXiv:1312.5000.

[50] G. J. Feldman and R. D. Cousins, *A unified approach to the classical statistical analysis of small signals*, Phys. Rev. **D57** (1998) 3873, arXiv:physics/9711021.

[51] LHCb collaboration, R. Aaij *et al.*, *Observation of the decay $B_c^+ \to \psi(2S)\pi^+$*, Phys. Rev. **D87** (2013) 071103(R), arXiv:1303.1737.

[52] LHCb collaboration, R. Aaij *et al.*, *Measurement of the branching fraction ratio $\mathcal{B}(B_c^+ \to \psi(2S)\pi^+)/\mathcal{B}(B_c^+ \to J/\psi\pi^+)$*, Phys. Rev. **D92** (2015) 057007, arXiv:1507.03516.

LHCb collaboration

R. Aaij[36], A.S.W. Abdelmotteleb[55], C. Abellan Beteta[49], F. Abudinén[55], T. Ackernley[59], A. A. Adefisoye[67], B. Adeva[45], M. Adinolfi[53], P. Adlarson[80], C. Agapopoulou[13], C.A. Aidala[81], Z. Ajaltouni[11], S. Akar[64], K. Akiba[36], P. Albicocco[26], J. Albrecht[18], F. Alessio[47], M. Alexander[58], Z. Aliouche[61], P. Alvarez Cartelle[54], R. Amalric[15], S. Amato[3], J.L. Amey[53], Y. Amhis[13,47], L. An[6], L. Anderlini[25], M. Andersson[49], A. Andreianov[42], P. Andreola[49], M. Andreotti[24], D. Andreou[67], A. Anelli[29,n], D. Ao[7], F. Archilli[35,t], M. Argenton[24], S. Arguedas Cuendis[9,47], A. Artamonov[42], M. Artuso[67], E. Aslanides[12], R. Ataíde Da Silva[48], M. Atzeni[63], B. Audurier[14], D. Bacher[62], I. Bachiller Perea[10], S. Bachmann[20], M. Bachmayer[48], J.J. Back[55], P. Baladron Rodriguez[45], V. Balagura[14], W. Baldini[24], L. Balzani[18], H. Bao[7], J. Baptista de Souza Leite[59], C. Barbero Pretel[45,82], M. Barbetti[25], I. R. Barbosa[68], R.J. Barlow[61], M. Barnyakov[23], S. Barsuk[13], W. Barter[57], M. Bartolini[54], J. Bartz[67], J.M. Basels[16], S. Bashir[38], G. Bassi[33,q], B. Batsukh[5], P. B. Battista[13], A. Bay[48], A. Beck[55], M. Becker[18], F. Bedeschi[33], I.B. Bediaga[2], N. A. Behling[18], S. Belin[45], V. Bellee[49], K. Belous[42], I. Belov[27], I. Belyaev[34], G. Benane[12], G. Bencivenni[26], E. Ben-Haim[15], A. Berezhnoy[42], R. Bernet[49], S. Bernet Andres[43], A. Bertolin[31], C. Betancourt[49], F. Betti[57], J. Bex[54], Ia. Bezshyiko[49], J. Bhom[39], M.S. Bieker[18], N.V. Biesuz[24], P. Billoir[15], A. Biolchini[36], M. Birch[60], F.C.R. Bishop[10], A. Bitadze[61], A. Bizzeti, T. Blake[55], F. Blanc[48], J.E. Blank[18], S. Blusk[67], V. Bocharnikov[42], J.A. Boelhauve[18], O. Boente Garcia[14], T. Boettcher[64], A. Bohare[57], A. Boldyrev[42], C.S. Bolognani[77], R. Bolzonella[24,k], N. Bondar[42], A. Bordelius[47], F. Borgato[31,o], S. Borghi[61], M. Borsato[29,n], J.T. Borsuk[39], S.A. Bouchiba[48], M. Bovill[62], T.J.V. Bowcock[59], A. Boyer[47], C. Bozzi[24], A. Brea Rodriguez[48], N. Breer[18], J. Brodzicka[39], A. Brossa Gonzalo[45,55,44,†], J. Brown[59], D. Brundu[30], E. Buchanan[57], A. Buonaura[49], L. Buonincontri[31,o], A.T. Burke[61], C. Burr[47], A. Butkevich[42], J.S. Butter[54], J. Buytaert[47], W. Byczynski[47], S. Cadeddu[30], H. Cai[72], A. C. Caillet[15], R. Calabrese[24,k], S. Calderon Ramirez[9], L. Calefice[44], S. Cali[26], M. Calvi[29,n], M. Calvo Gomez[43], P. Camargo Magalhaes[2,x], J. I. Cambon Bouzas[45], P. Campana[26], D.H. Campora Perez[77], A.F. Campoverde Quezada[7], S. Capelli[29], L. Capriotti[24], R. Caravaca-Mora[9], A. Carbone[23,i], L. Carcedo Salgado[45], R. Cardinale[27,l], A. Cardini[30], P. Carniti[29,n], L. Carus[20], A. Casais Vidal[63], R. Caspary[20], G. Casse[59], J. Castro Godinez[9], M. Cattaneo[47], G. Cavallero[24,47], V. Cavallini[24,k], S. Celani[20], D. Cervenkov[62], S. Cesare[28,m], A.J. Chadwick[59], I. Chahrour[81], M. Charles[15], Ph. Charpentier[47], E. Chatzianagnostou[36], C.A. Chavez Barajas[59], M. Chefdeville[10], C. Chen[12], S. Chen[5], Z. Chen[7], A. Chernov[39], S. Chernyshenko[51], X. Chiotopoulos[77], V. Chobanova[79], S. Cholak[48], M. Chrzaszcz[39], A. Chubykin[42], V. Chulikov[42], P. Ciambrone[26], X. Cid Vidal[45], G. Ciezarek[47], P. Cifra[47], P.E.L. Clarke[57], M. Clemencic[47], H.V. Cliff[54], J. Closier[47], C. Cocha Toapaxi[20], V. Coco[47], J. Cogan[12], E. Cogneras[11], L. Cojocariu[41], P. Collins[47], T. Colombo[47], M. C. Colonna[18], A. Comerma-Montells[44], L. Congedo[22], A. Contu[30], N. Cooke[58], I. Corredoira [45], A. Correia[15], G. Corti[47], J.J. Cottee Meldrum[53], B. Couturier[47], D.C. Craik[49], M. Cruz Torres[2,f], E. Curras Rivera[48], R. Currie[57], C.L. Da Silva[66], S. Dadabaev[42], L. Dai[69], X. Dai[6], E. Dall'Occo[18], J. Dalseno[45], C. D'Ambrosio[47], J. Daniel[11], A. Danilina[42], P. d'Argent[22], A. Davidson[55], J.E. Davies[61], A. Davis[61], O. De Aguiar Francisco[61], C. De Angelis[30,j],

F. De Benedetti[47], J. de Boer[36], K. De Bruyn[76], S. De Capua[61], M. De Cian[20,47], U. De Freitas Carneiro Da Graca[2,b], E. De Lucia[26], J.M. De Miranda[2], L. De Paula[3], M. De Serio[22,g], P. De Simone[26], F. De Vellis[18], J.A. de Vries[77], S. Deacon[55], F. Debernardis[22], D. Decamp[10], V. Dedu[12], S. Dekkers[1], L. Del Buono[15], B. Delaney[63], H.-P. Dembinski[18], J. Deng[8], V. Denysenko[49], O. Deschamps[11], F. Dettori[30,j], B. Dey[75], P. Di Nezza[26], I. Diachkov[42], S. Didenko[42], S. Ding[67], L. Dittmann[20], V. Dobishuk[51], A. D. Docheva[58], C. Dong[4], A.M. Donohoe[21], F. Dordei[30], A.C. dos Reis[2], A. D. Dowling[67], W. Duan[70], P. Duda[78], M.W. Dudek[39], L. Dufour[47], V. Duk[32], P. Durante[47], M. M. Duras[78], J.M. Durham[66], O. D. Durmus[75], A. Dziurda[39], A. Dzyuba[42], S. Easo[56], E. Eckstein[17], U. Egede[1], A. Egorychev[42], V. Egorychev[42], S. Eisenhardt[57], E. Ejopu[61], L. Eklund[80], M. Elashri[64], J. Ellbracht[18], S. Ely[60], A. Ene[41], E. Epple[64], J. Eschle[67], S. Esen[20], T. Evans[61], F. Fabiano[30,j], L.N. Falcao[2], Y. Fan[7], B. Fang[72], L. Fantini[32,p,47], M. Faria[48], K. Farmer[57], D. Fazzini[29,n], L. Felkowski[78], M. Feng[5,7], M. Feo[18,47], A. Fernandez Casani[46], M. Fernandez Gomez[45], A.D. Fernez[65], F. Ferrari[23], F. Ferreira Rodrigues[3], M. Ferrillo[49], M. Ferro-Luzzi[47], S. Filippov[42], R.A. Fini[22], M. Fiorini[24,k], K.L. Fischer[62], D.S. Fitzgerald[81], C. Fitzpatrick[61], F. Fleuret[14], M. Fontana[23], L. F. Foreman[61], R. Forty[47], D. Foulds-Holt[54], V. Franco Lima[3], M. Franco Sevilla[65], M. Frank[47], E. Franzoso[24,k], G. Frau[61], C. Frei[47], D.A. Friday[61], J. Fu[7], Q. Fuehring[18,54], Y. Fujii[1], T. Fulghesu[15], E. Gabriel[36], G. Galati[22], M.D. Galati[36], A. Gallas Torreira[45], D. Galli[23,i], S. Gambetta[57], M. Gandelman[3], P. Gandini[28], B. Ganie[61], H. Gao[7], R. Gao[62], T.Q. Gao[54], Y. Gao[8], Y. Gao[6], Y. Gao[8], M. Garau[30,j], L.M. Garcia Martin[48], P. Garcia Moreno[44], J. García Pardiñas[47], K. G. Garg[8], L. Garrido[44], C. Gaspar[47], R.E. Geertsema[36], L.L. Gerken[18], E. Gersabeck[61], M. Gersabeck[61], T. Gershon[55], S. G. Ghizzo[27,l], Z. Ghorbanimoghaddam[53], L. Giambastiani[31,o], F. I. Giasemis[15,e], V. Gibson[54], H.K. Giemza[40], A.L. Gilman[62], M. Giovannetti[26], A. Gioventù[44], L. Girardey[61], P. Gironella Gironell[44], C. Giugliano[24,k], M.A. Giza[39], E.L. Gkougkousis[60], F.C. Glaser[13,20], V.V. Gligorov[15,47], C. Göbel[68], E. Golobardes[43], D. Golubkov[42], A. Golutvin[60,42,47], A. Gomes[2,a,†], S. Gomez Fernandez[44], F. Goncalves Abrantes[62], M. Goncerz[39], G. Gong[4], J. A. Gooding[18], I.V. Gorelov[42], C. Gotti[29], J.P. Grabowski[17], L.A. Granado Cardoso[47], E. Graugés[44], E. Graverini[48,r], L. Grazette[55], G. Graziani, A. T. Grecu[41], L.M. Greeven[36], N.A. Grieser[64], L. Grillo[58], S. Gromov[42], C. Gu[14], M. Guarise[24], L. Guerry[11], M. Guittiere[13], V. Guliaeva[42], P. A. Günther[20], A.-K. Guseinov[48], E. Gushchin[42], Y. Guz[6,42,47], T. Gys[47], K. Habermann[17], T. Hadavizadeh[1], C. Hadjivasiliou[65], G. Haefeli[48], C. Haen[47], J. Haimberger[47], M. Hajheidari[47], G. Hallett[55], M.M. Halvorsen[47], P.M. Hamilton[65], J. Hammerich[59], Q. Han[8], X. Han[20], S. Hansmann-Menzemer[20], L. Hao[7], N. Harnew[62], M. Hartmann[13], S. Hashmi[38], J. He[7,c], F. Hemmer[47], C. Henderson[64], R.D.L. Henderson[1,55], A.M. Hennequin[47], K. Hennessy[59], L. Henry[48], J. Herd[60], P. Herrero Gascon[20], J. Heuel[16], A. Hicheur[3], G. Hijano Mendizabal[49], D. Hill[48], S.E. Hollitt[18], J. Horswill[61], R. Hou[8], Y. Hou[11], N. Howarth[59], J. Hu[20], J. Hu[70], W. Hu[6], X. Hu[4], W. Huang[7], W. Hulsbergen[36], R.J. Hunter[55], M. Hushchyn[42], D. Hutchcroft[59], D. Ilin[42], P. Ilten[64], A. Inglessi[42], A. Iniukhin[42], A. Ishteev[42], K. Ivshin[42], R. Jacobsson[47], H. Jage[16], S.J. Jaimes Elles[46,73], S. Jakobsen[47], E. Jans[36], B.K. Jashal[46], A. Jawahery[65,47], V. Jevtic[18], E. Jiang[65], X. Jiang[5,7], Y. Jiang[7], Y. J. Jiang[6], M. John[62], A. John Rubesh Rajan[21], D. Johnson[52], C.R. Jones[54], T.P. Jones[55], S. Joshi[40], B. Jost[47], J. Juan Castella[54], N. Jurik[47], I. Juszczak[39], D. Kaminaris[48],

S. Kandybei[50], M. Kane[57], Y. Kang[4], C. Kar[11], M. Karacson[47], D. Karpenkov[42], A. Kauniskangas[48], J.W. Kautz[64], M.K. Kazanecki[39], F. Keizer[47], M. Kenzie[54], T. Ketel[36], B. Khanji[67], A. Kharisova[42], S. Kholodenko[33,47], G. Khreich[13], T. Kirn[16], V.S. Kirsebom[29,n], O. Kitouni[63], S. Klaver[37], N. Kleijne[33,q], K. Klimaszewski[40], M.R. Kmiec[40], S. Koliiev[51], L. Kolk[18], A. Konoplyannikov[42], P. Kopciewicz[38,47], P. Koppenburg[36], M. Korolev[42], I. Kostiuk[36], O. Kot[51], S. Kotriakhova, A. Kozachuk[42], P. Kravchenko[42], L. Kravchuk[42], M. Kreps[55], P. Krokovny[42], W. Krupa[67], W. Krzemien[40], O.K. Kshyvanskyi[51], J. Kubat[20], S. Kubis[78], M. Kucharczyk[39], V. Kudryavtsev[42], E. Kulikova[42], A. Kupsc[80], B. K. Kutsenko[12], D. Lacarrere[47], P. Laguarta Gonzalez[44], A. Lai[30], A. Lampis[30], D. Lancierini[54], C. Landesa Gomez[45], J.J. Lane[1], R. Lane[53], G. Lanfranchi[26], C. Langenbruch[20], J. Langer[18], O. Lantwin[42], T. Latham[55], F. Lazzari[33,r], C. Lazzeroni[52], R. Le Gac[12], H. Lee[59], R. Lefèvre[11], A. Leflat[42], S. Legotin[42], M. Lehuraux[55], E. Lemos Cid[47], O. Leroy[12], T. Lesiak[39], E. Lesser[47], B. Leverington[20], A. Li[4], C. Li[12], H. Li[70], K. Li[8], L. Li[61], P. Li[7], P.-R. Li[71], Q. Li[5,7], S. Li[8], T. Li[5,d], T. Li[70], Y. Li[8], Y. Li[5], Z. Lian[4], X. Liang[67], S. Libralon[46], C. Lin[7], T. Lin[56], R. Lindner[47], V. Lisovskyi[48], R. Litvinov[30,47], F. L. Liu[1], G. Liu[70], K. Liu[71], S. Liu[5,7], W. Liu[8], Y. Liu[57], Y. Liu[71], Y. L. Liu[60], A. Lobo Salvia[44], A. Loi[30], J. Lomba Castro[45], T. Long[54], J.H. Lopes[3], A. Lopez Huertas[44], S. López Soliño[45], Q. Lu[14], C. Lucarelli[25], D. Lucchesi[31,o], M. Lucio Martinez[77], V. Lukashenko[36,51], Y. Luo[6], A. Lupato[31,h], E. Luppi[24,k], K. Lynch[21], X.-R. Lyu[7], G. M. Ma[4], R. Ma[7], S. Maccolini[18], F. Machefert[13], F. Maciuc[41], B. Mack[67], I. Mackay[62], L. M. Mackey[67], L.R. Madhan Mohan[54], M.J. Madurai[52], A. Maevskiy[42], D. Magdalinski[36], V. Mahajan[55], D. Maisuzenko[42], M.W. Majewski[38], J.J. Malczewski[39], S. Malde[62], L. Malentacca[47], A. Malinin[42], T. Maltsev[42], G. Manca[30,j], G. Mancinelli[12], C. Mancuso[28,13,m], R. Manera Escalero[44], D. Manuzzi[23], D. Marangotto[28,m], J.F. Marchand[10], R. Marchevski[48], U. Marconi[23], E. Mariani[15], S. Mariani[47], C. Marin Benito[44], J. Marks[20], A.M. Marshall[53], L. Martel[62], G. Martelli[32,p], G. Martellotti[34], L. Martinazzoli[47], M. Martinelli[29,n], D. Martinez Santos[45], F. Martinez Vidal[46], A. Massafferri[2], R. Matev[47], A. Mathad[47], V. Matiunin[42], C. Matteuzzi[67], K.R. Mattioli[14], A. Mauri[60], E. Maurice[14], J. Mauricio[44], P. Mayencourt[48], J. Mazorra de Cos[46], M. Mazurek[40], M. McCann[60], L. Mcconnell[21], T.H. McGrath[61], N.T. McHugh[58], A. McNab[61], R. McNulty[21], B. Meadows[64], G. Meier[18], D. Melnychuk[40], F. M. Meng[4], M. Merk[36,77], A. Merli[48], L. Meyer Garcia[65], D. Miao[5,7], H. Miao[7], M. Mikhasenko[74], D.A. Milanes[73], A. Minotti[29,n], E. Minucci[67], T. Miralles[11], B. Mitreska[18], D.S. Mitzel[18], A. Modak[56], R.A. Mohammed[62], R.D. Moise[16], S. Mokhnenko[42], E. F. Molina Cardenas[81], T. Mombächer[47], M. Monk[55,1], S. Monteil[11], A. Morcillo Gomez[45], G. Morello[26], M.J. Morello[33,q], M.P. Morgenthaler[20], A.B. Morris[47], A.G. Morris[12], R. Mountain[67], H. Mu[4], Z. M. Mu[6], E. Muhammad[55], F. Muheim[57], M. Mulder[76], K. Müller[49], F. Muñoz-Rojas[9], R. Murta[60], P. Naik[59], T. Nakada[48], R. Nandakumar[56], T. Nanut[47], I. Nasteva[3], M. Needham[57], N. Neri[28,m], S. Neubert[17], N. Neufeld[47], P. Neustroev[42], J. Nicolini[18,13], D. Nicotra[77], E.M. Niel[48], N. Nikitin[42], P. Nogarolli[3], P. Nogga[17], N.S. Nolte[63], C. Normand[53], J. Novoa Fernandez[45], G. Nowak[64], C. Nunez[81], H. N. Nur[58], A. Oblakowska-Mucha[38], V. Obraztsov[42], T. Oeser[16], S. Okamura[24,k], A. Okhotnikov[42], O. Okhrimenko[51], R. Oldeman[30,j], F. Oliva[57], M. Olocco[18], C.J.G. Onderwater[77], R.H. O'Neil[57], D. Osthues[18], J.M. Otalora Goicochea[3], P. Owen[49], A. Oyanguren[46], O. Ozcelik[57], F. Paciolla[33,u],

A. Padee[40], K.O. Padeken[17], B. Pagare[55], P.R. Pais[20], T. Pajero[47], A. Palano[22], M. Palutan[26], G. Panshin[42], L. Paolucci[55], A. Papanestis[56], M. Pappagallo[22,g], L.L. Pappalardo[24,k], C. Pappenheimer[64], C. Parkes[61], B. Passalacqua[24], G. Passaleva[25], D. Passaro[33,q], A. Pastore[22], M. Patel[60], J. Patoc[62], C. Patrignani[23,i], A. Paul[67], C.J. Pawley[77], A. Pellegrino[36], J. Peng[5,7], M. Pepe Altarelli[26], S. Perazzini[23], D. Pereima[42], H. Pereira Da Costa[66], A. Pereiro Castro[45], P. Perret[11], A. Perro[47], K. Petridis[53], A. Petrolini[27,l], J. P. Pfaller[64], H. Pham[67], L. Pica[33,q], M. Piccini[32], B. Pietrzyk[10], G. Pietrzyk[13], D. Pinci[34], F. Pisani[47], M. Pizzichemi[29,n,47], V. Placinta[41], M. Plo Casasus[45], T. Poeschl[47], F. Polci[15,47], M. Poli Lener[26], A. Poluektov[12], N. Polukhina[42], I. Polyakov[47], E. Polycarpo[3], S. Ponce[47], D. Popov[7], S. Poslavskii[42], K. Prasanth[57], C. Prouve[45], V. Pugatch[51], G. Punzi[33,r], S. Qasim[49], Q. Q. Qian[6], W. Qian[7], N. Qin[4], S. Qu[4], R. Quagliani[47], R.I. Rabadan Trejo[55], J.H. Rademacker[53], M. Rama[33], M. Ramírez García[81], V. Ramos De Oliveira[68], M. Ramos Pernas[55], M.S. Rangel[3], F. Ratnikov[42], G. Raven[37], M. Rebollo De Miguel[46], F. Redi[28,h], J. Reich[53], F. Reiss[61], Z. Ren[7], P.K. Resmi[62], R. Ribatti[48], G. R. Ricart[14,82], D. Riccardi[33,q], S. Ricciardi[56], K. Richardson[63], M. Richardson-Slipper[57], K. Rinnert[59], P. Robbe[13], G. Robertson[58], E. Rodrigues[59], E. Rodriguez Fernandez[45], J.A. Rodriguez Lopez[73], E. Rodriguez Rodriguez[45], J. Roensch[18], A. Rogachev[42], A. Rogovskiy[56], D.L. Rolf[47], P. Roloff[47], V. Romanovskiy[42], M. Romero Lamas[45], A. Romero Vidal[45], G. Romolini[24], F. Ronchetti[48], T. Rong[6], M. Rotondo[26], S. R. Roy[20], M.S. Rudolph[67], M. Ruiz Diaz[20], R.A. Ruiz Fernandez[45], J. Ruiz Vidal[80,y], A. Ryzhikov[42], J. Ryzka[38], J. J. Saavedra-Arias[9], J.J. Saborido Silva[45], R. Sadek[14], N. Sagidova[42], D. Sahoo[75], N. Sahoo[52], B. Saitta[30,j], M. Salomoni[29,47,n], C. Sanchez Gras[36], I. Sanderswood[46], R. Santacesaria[34], C. Santamarina Rios[45], M. Santimaria[26,47], L. Santoro [2], E. Santovetti[35], A. Saputi[24,47], D. Saranin[42], A. Sarnatskiy[76], G. Sarpis[57], M. Sarpis[61], C. Satriano[34,s], A. Satta[35], M. Saur[6], D. Savrina[42], H. Sazak[16], F. Sborzacchi[47,26], L.G. Scantlebury Smead[62], A. Scarabotto[18], S. Schael[16], S. Scherl[59], M. Schiller[58], H. Schindler[47], M. Schmelling[19], B. Schmidt[47], S. Schmitt[16], H. Schmitz[17], O. Schneider[48], A. Schopper[47], N. Schulte[18], S. Schulte[48], M.H. Schune[13], R. Schwemmer[47], G. Schwering[16], B. Sciascia[26], A. Sciuccati[47], S. Sellam[45], A. Semennikov[42], T. Senger[49], M. Senghi Soares[37], A. Sergi[27,l,47], N. Serra[49], L. Sestini[31], A. Seuthe[18], Y. Shang[6], D.M. Shangase[81], M. Shapkin[42], R. S. Sharma[67], I. Shchemerov[42], L. Shchutska[48], T. Shears[59], L. Shekhtman[42], Z. Shen[6], S. Sheng[5,7], V. Shevchenko[42], B. Shi[7], Q. Shi[7], Y. Shimizu[13], E. Shmanin[42], R. Shorkin[42], J.D. Shupperd[67], R. Silva Coutinho[67], G. Simi[31,o], S. Simone[22,g], N. Skidmore[55], T. Skwarnicki[67], M.W. Slater[52], J.C. Smallwood[62], E. Smith[63], K. Smith[66], M. Smith[60], A. Snoch[36], L. Soares Lavra[57], M.D. Sokoloff[64], F.J.P. Soler[58], A. Solomin[42,53], A. Solovev[42], I. Solovyev[42], R. Song[1], Y. Song[48], Y. Song[4], Y. S. Song[6], F.L. Souza De Almeida[67], B. Souza De Paula[3], E. Spadaro Norella[27,l], E. Spedicato[23], J.G. Speer[18], E. Spiridenkov[42], P. Spradlin[58], V. Sriskaran[47], F. Stagni[47], M. Stahl[47], S. Stahl[47], S. Stanislaus[62], E.N. Stein[47], O. Steinkamp[49], O. Stenyakin[42], H. Stevens[18], D. Strekalina[42], Y. Su[7], F. Suljik[62], J. Sun[30], L. Sun[72], Y. Sun[65], D. Sundfeld[2], W. Sutcliffe[49], P.N. Swallow[52], F. Swystun[54], A. Szabelski[40], T. Szumlak[38], Y. Tan[4], M.D. Tat[62], A. Terentev[42], F. Terzuoli[33,u,47], F. Teubert[47], E. Thomas[47], D.J.D. Thompson[52], H. Tilquin[60], V. Tisserand[11], S. T'Jampens[10], M. Tobin[5,47], L. Tomassetti[24,k], G. Tonani[28,m,47], X. Tong[6], D. Torres Machado[2], L. Toscano[18], D.Y. Tou[4], C. Trippl[43], G. Tuci[20],

N. Tuning[36], L.H. Uecker[20], A. Ukleja[38], D.J. Unverzagt[20], E. Ursov[42], A. Usachov[37], A. Ustyuzhanin[42], U. Uwer[20], V. Vagnoni[23], V. Valcarce Cadenas[45], G. Valenti[23], N. Valls Canudas[47], H. Van Hecke[66], E. van Herwijnen[60], C.B. Van Hulse[45,w], R. Van Laak[48], M. van Veghel[36], G. Vasquez[49], R. Vazquez Gomez[44], P. Vazquez Regueiro[45], C. Vázquez Sierra[45], S. Vecchi[24], J.J. Velthuis[53], M. Veltri[25,v], A. Venkateswaran[48], M. Vesterinen[55], D. Vico Benet[62], P. V. Vidrier Villalba[44], M. Vieites Diaz[47], X. Vilasis-Cardona[43], E. Vilella Figueras[59], A. Villa[23], P. Vincent[15], F.C. Volle[52], D. vom Bruch[12], N. Voropaev[42], K. Vos[77], G. Vouters[10,47], C. Vrahas[57], J. Wagner[18], J. Walsh[33], E.J. Walton[1,55], G. Wan[6], C. Wang[20], G. Wang[8], J. Wang[6], J. Wang[5], J. Wang[4], J. Wang[72], M. Wang[28], N. W. Wang[7], R. Wang[53], X. Wang[8], X. Wang[70], X. W. Wang[60], Y. Wang[6], Z. Wang[13], Z. Wang[4], Z. Wang[28], J.A. Ward[55,1], M. Waterlaat[47], N.K. Watson[52], D. Websdale[60], Y. Wei[6], J. Wendel[79], B.D.C. Westhenry[53], C. White[54], M. Whitehead[58], E. Whiter[52], A.R. Wiederhold[61], D. Wiedner[18], G. Wilkinson[62], M.K. Wilkinson[64], M. Williams[63], M.R.J. Williams[57], R. Williams[54], Z. Williams[53], F.F. Wilson[56], W. Wislicki[40], M. Witek[39], L. Witola[20], G. Wormser[13], S.A. Wotton[54], H. Wu[67], J. Wu[8], Y. Wu[6], Z. Wu[7], K. Wyllie[47], S. Xian[70], Z. Xiang[5], Y. Xie[8], A. Xu[33], J. Xu[7], L. Xu[4], L. Xu[4], M. Xu[55], Z. Xu[47], Z. Xu[7], Z. Xu[5], D. Yang, K. Yang[60], S. Yang[7], X. Yang[6], Y. Yang[27,l], Z. Yang[6], Z. Yang[65], V. Yeroshenko[13], H. Yeung[61], H. Yin[8], C. Y. Yu[6], J. Yu[69], X. Yuan[5], Y Yuan[5,7], E. Zaffaroni[48], M. Zavertyaev[19], M. Zdybal[39], F. Zenesini[23,i], C. Zeng[5,7], M. Zeng[4], C. Zhang[6], D. Zhang[8], J. Zhang[7], L. Zhang[4], S. Zhang[69], S. Zhang[62], Y. Zhang[6], Y. Z. Zhang[4], Y. Zhao[20], A. Zharkova[42], A. Zhelezov[20], S. Z. Zheng[6], X. Z. Zheng[4], Y. Zheng[7], T. Zhou[6], X. Zhou[8], Y. Zhou[7], V. Zhovkovska[55], L. Z. Zhu[7], X. Zhu[4], X. Zhu[8], V. Zhukov[16], J. Zhuo[46], Q. Zou[5,7], D. Zuliani[31,o], G. Zunica[48].

[1] *School of Physics and Astronomy, Monash University, Melbourne, Australia*
[2] *Centro Brasileiro de Pesquisas Físicas (CBPF), Rio de Janeiro, Brazil*
[3] *Universidade Federal do Rio de Janeiro (UFRJ), Rio de Janeiro, Brazil*
[4] *Center for High Energy Physics, Tsinghua University, Beijing, China*
[5] *Institute Of High Energy Physics (IHEP), Beijing, China*
[6] *School of Physics State Key Laboratory of Nuclear Physics and Technology, Peking University, Beijing, China*
[7] *University of Chinese Academy of Sciences, Beijing, China*
[8] *Institute of Particle Physics, Central China Normal University, Wuhan, Hubei, China*
[9] *Consejo Nacional de Rectores (CONARE), San Jose, Costa Rica*
[10] *Université Savoie Mont Blanc, CNRS, IN2P3-LAPP, Annecy, France*
[11] *Université Clermont Auvergne, CNRS/IN2P3, LPC, Clermont-Ferrand, France*
[12] *Aix Marseille Univ, CNRS/IN2P3, CPPM, Marseille, France*
[13] *Université Paris-Saclay, CNRS/IN2P3, IJCLab, Orsay, France*
[14] *Laboratoire Leprince-Ringuet, CNRS/IN2P3, Ecole Polytechnique, Institut Polytechnique de Paris, Palaiseau, France*
[15] *LPNHE, Sorbonne Université, Paris Diderot Sorbonne Paris Cité, CNRS/IN2P3, Paris, France*
[16] *I. Physikalisches Institut, RWTH Aachen University, Aachen, Germany*
[17] *Universität Bonn - Helmholtz-Institut für Strahlen und Kernphysik, Bonn, Germany*
[18] *Fakultät Physik, Technische Universität Dortmund, Dortmund, Germany*
[19] *Max-Planck-Institut für Kernphysik (MPIK), Heidelberg, Germany*
[20] *Physikalisches Institut, Ruprecht-Karls-Universität Heidelberg, Heidelberg, Germany*
[21] *School of Physics, University College Dublin, Dublin, Ireland*
[22] *INFN Sezione di Bari, Bari, Italy*
[23] *INFN Sezione di Bologna, Bologna, Italy*

[24] *INFN Sezione di Ferrara, Ferrara, Italy*
[25] *INFN Sezione di Firenze, Firenze, Italy*
[26] *INFN Laboratori Nazionali di Frascati, Frascati, Italy*
[27] *INFN Sezione di Genova, Genova, Italy*
[28] *INFN Sezione di Milano, Milano, Italy*
[29] *INFN Sezione di Milano-Bicocca, Milano, Italy*
[30] *INFN Sezione di Cagliari, Monserrato, Italy*
[31] *INFN Sezione di Padova, Padova, Italy*
[32] *INFN Sezione di Perugia, Perugia, Italy*
[33] *INFN Sezione di Pisa, Pisa, Italy*
[34] *INFN Sezione di Roma La Sapienza, Roma, Italy*
[35] *INFN Sezione di Roma Tor Vergata, Roma, Italy*
[36] *Nikhef National Institute for Subatomic Physics, Amsterdam, Netherlands*
[37] *Nikhef National Institute for Subatomic Physics and VU University Amsterdam, Amsterdam, Netherlands*
[38] *AGH - University of Krakow, Faculty of Physics and Applied Computer Science, Kraków, Poland*
[39] *Henryk Niewodniczanski Institute of Nuclear Physics Polish Academy of Sciences, Kraków, Poland*
[40] *National Center for Nuclear Research (NCBJ), Warsaw, Poland*
[41] *Horia Hulubei National Institute of Physics and Nuclear Engineering, Bucharest-Magurele, Romania*
[42] *Affiliated with an institute covered by a cooperation agreement with CERN*
[43] *DS4DS, La Salle, Universitat Ramon Llull, Barcelona, Spain*
[44] *ICCUB, Universitat de Barcelona, Barcelona, Spain*
[45] *Instituto Galego de Física de Altas Enerxías (IGFAE), Universidade de Santiago de Compostela, Santiago de Compostela, Spain*
[46] *Instituto de Fisica Corpuscular, Centro Mixto Universidad de Valencia - CSIC, Valencia, Spain*
[47] *European Organization for Nuclear Research (CERN), Geneva, Switzerland*
[48] *Institute of Physics, Ecole Polytechnique Fédérale de Lausanne (EPFL), Lausanne, Switzerland*
[49] *Physik-Institut, Universität Zürich, Zürich, Switzerland*
[50] *NSC Kharkiv Institute of Physics and Technology (NSC KIPT), Kharkiv, Ukraine*
[51] *Institute for Nuclear Research of the National Academy of Sciences (KINR), Kyiv, Ukraine*
[52] *School of Physics and Astronomy, University of Birmingham, Birmingham, United Kingdom*
[53] *H.H. Wills Physics Laboratory, University of Bristol, Bristol, United Kingdom*
[54] *Cavendish Laboratory, University of Cambridge, Cambridge, United Kingdom*
[55] *Department of Physics, University of Warwick, Coventry, United Kingdom*
[56] *STFC Rutherford Appleton Laboratory, Didcot, United Kingdom*
[57] *School of Physics and Astronomy, University of Edinburgh, Edinburgh, United Kingdom*
[58] *School of Physics and Astronomy, University of Glasgow, Glasgow, United Kingdom*
[59] *Oliver Lodge Laboratory, University of Liverpool, Liverpool, United Kingdom*
[60] *Imperial College London, London, United Kingdom*
[61] *Department of Physics and Astronomy, University of Manchester, Manchester, United Kingdom*
[62] *Department of Physics, University of Oxford, Oxford, United Kingdom*
[63] *Massachusetts Institute of Technology, Cambridge, MA, United States*
[64] *University of Cincinnati, Cincinnati, OH, United States*
[65] *University of Maryland, College Park, MD, United States*
[66] *Los Alamos National Laboratory (LANL), Los Alamos, NM, United States*
[67] *Syracuse University, Syracuse, NY, United States*
[68] *Pontifícia Universidade Católica do Rio de Janeiro (PUC-Rio), Rio de Janeiro, Brazil, associated to* [3]
[69] *School of Physics and Electronics, Hunan University, Changsha City, China, associated to* [8]
[70] *Guangdong Provincial Key Laboratory of Nuclear Science, Guangdong-Hong Kong Joint Laboratory of Quantum Matter, Institute of Quantum Matter, South China Normal University, Guangzhou, China, associated to* [4]
[71] *Lanzhou University, Lanzhou, China, associated to* [5]
[72] *School of Physics and Technology, Wuhan University, Wuhan, China, associated to* [4]
[73] *Departamento de Fisica, Universidad Nacional de Colombia, Bogota, Colombia, associated to* [15]
[74] *Ruhr Universitaet Bochum, Fakultaet f. Physik und Astronomie, Bochum, Germany, associated to* [18]
[75] *Eotvos Lorand University, Budapest, Hungary, associated to* [47]

[76] *Van Swinderen Institute, University of Groningen, Groningen, Netherlands, associated to* [36]
[77] *Universiteit Maastricht, Maastricht, Netherlands, associated to* [36]
[78] *Tadeusz Kosciuszko Cracow University of Technology, Cracow, Poland, associated to* [39]
[79] *Universidade da Coruña, A Coruna, Spain, associated to* [43]
[80] *Department of Physics and Astronomy, Uppsala University, Uppsala, Sweden, associated to* [58]
[81] *University of Michigan, Ann Arbor, MI, United States, associated to* [67]
[82] *Département de Physique Nucléaire (DPhN), Gif-Sur-Yvette, France*

[a] *Universidade de Brasília, Brasília, Brazil*
[b] *Centro Federal de Educacão Tecnológica Celso Suckow da Fonseca, Rio De Janeiro, Brazil*
[c] *Hangzhou Institute for Advanced Study, UCAS, Hangzhou, China*
[d] *School of Physics and Electronics, Henan University, Kaifeng, China*
[e] *LIP6, Sorbonne Université, Paris, France*
[f] *Universidad Nacional Autónoma de Honduras, Tegucigalpa, Honduras*
[g] *Università di Bari, Bari, Italy*
[h] *Università di Bergamo, Bergamo, Italy*
[i] *Università di Bologna, Bologna, Italy*
[j] *Università di Cagliari, Cagliari, Italy*
[k] *Università di Ferrara, Ferrara, Italy*
[l] *Università di Genova, Genova, Italy*
[m] *Università degli Studi di Milano, Milano, Italy*
[n] *Università degli Studi di Milano-Bicocca, Milano, Italy*
[o] *Università di Padova, Padova, Italy*
[p] *Università di Perugia, Perugia, Italy*
[q] *Scuola Normale Superiore, Pisa, Italy*
[r] *Università di Pisa, Pisa, Italy*
[s] *Università della Basilicata, Potenza, Italy*
[t] *Università di Roma Tor Vergata, Roma, Italy*
[u] *Università di Siena, Siena, Italy*
[v] *Università di Urbino, Urbino, Italy*
[w] *Universidad de Alcalá, Alcalá de Henares, Spain*
[x] *Facultad de Ciencias Fisicas, Madrid, Spain*
[y] *Department of Physics/Division of Particle Physics, Lund, Sweden*

[†] *Deceased*